



Simulation of fault dynamic rupture and near-field strong motion

Qifang Liu¹, Yifan Yuan², Xin Jin³

SUMMARY

Dynamic rupture process of earthquake fault and its near-field strong ground motions are simulated by time-space-decoupled, explicit finite element method with multi-transmitting formula (MTF) of artificial boundary in this paper. This decoupled, explicit method has advantage to easily incorporate into time-step simulation of dynamic rupture process on earthquake fault, as well as wave motions. The MTF approach for artificial boundary allows of performing simulation in a smaller computational model. Consequently, simulation can be implemented conveniently, say by microcomputer, resulted from substantially reduction of computational storage and time. It is meaningful for simulation of dynamic rupture of earthquake fault and its near-field motions, especially for high frequency motions, which is interested in earthquake engineering. Further, we use this method and slip-weakening frictional model to study the effect of different slip weakening distance d_c on the source time function, near filed ground motion and their Fourier spectra. It is found that d_c have little effect on the source time function and near filed ground motion for low frequency components ($<1\text{Hz}$).

INTRODUCTION

In recent earthquakes, such as the 1994 Northridge, 1995 Kobe, 1999 Chi-Chi earthquake, severe damage along the fault and some interesting phenomena related to fault rupture process remind us that near-field ground motion, especially near-fault ground motion need further study. Near-field ground motion depends on various factors, including site conditions, surface topography, crystal structure, and earthquake source *etc.* However, for sites close to a fault, ground motion strongly depends on the rupture process of fault. Earthquake fault rupture process is usually modeled as a propagating stress relaxation over a finite fault and it is controlled by the heterogeneous distribution of the initial tectonic stress, yield stress, and dynamic frictional stress *etc.* Such earthquake models generally lead to nonlinear, mixed boundary value problems, and close-form theoretical solutions are only available for few idealized problems [5, 9]. For most cases, especially three-dimensional problems, numerical methods have to be adopted to solve them. Three methods, such as the boundary integral equation method [1, 11], the finite difference method [2, 10], and the finite element method [3, 4], have been widely used for numerical simulation of the fault rupture process.

¹ Dr. candidate, Institute of engineering mechanics, CEA, E-mail liuqifang@sina.com

² Prof., Institute of engineering mechanics, CEA

³ Prof., Institute of engineering mechanics, CEA

Since an earthquake fault is usually of large dimensions, and near-field ground motions always include many high frequency components, the discrete grids of numerical computation should be very small compared to the fault dimension in order to satisfy the stability condition and accuracy of numerical simulation. Therefore, the numerical simulation always involves hundreds to millions of degrees of freedom requiring parallel computation. We can reduce the computational cost and decrease the computational time by two approaches. One is the high efficiency algorithm that can save the computer storage, and the other is the appropriate artificial boundary that can minimize whole computational area. In this paper, we present a time-space-decoupled, explicit finite element method, incorporating multi-transmitting formula (MTF) dealing with artificial boundary, to simulate the rupture process and near-field ground motions. Using this numerical scheme, dynamic rupture and near-field motions of a vertical fault is simulated to show its efficiency. The effect of slip weakening distance d_c on source function and ground motion is also discussed.

FINITE ELEMENT METHOD

1 Fault model, basic equation and boundary condition

A fault model of this study is shown in Figure 1, where the plane ABCD is the ground surface, the quadrangle abcd located in plane ADEH is the earthquake fault plane, which may or may not intersect the ground surface. The plane DCGH, BCGF, ABFE, and EHGF are the artificial boundaries of numerical simulation. Here, we take axis X parallel to the initial tectonic stress and axis Y perpendicular to the fault plane.

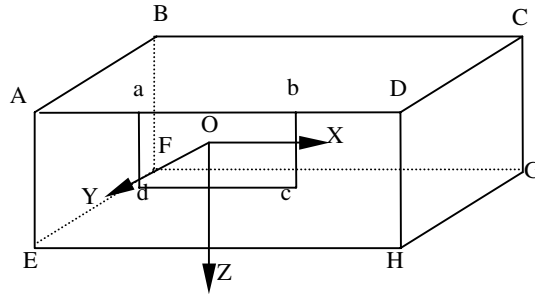


Figure 1 Geometry sketch of computational model with a fault embedded within a half-space.

It is well known, in elastic, isotropic, continuum medium, the displacement vector at any point should satisfy the following equation of motion,

$$\rho \ddot{u}_i = \lambda u_{k,k} \delta_{ij} + \mu (u_{i,jj} + u_{j,ii}) \quad (1)$$

where λ and μ are Lamé's constants, u denotes displacement, and ρ denotes mass density. The boundary condition on plane ADEH may be described in the following form,

On the fault plane ($y=0$), we have:

$$\tau_{yx} = -\tau_0 + \tau \quad (2)$$

$$\tau_{yz} = 0 \quad (3)$$

$$\tau_{yy} = 0 \quad (4)$$

where τ is the actual stress at time t , which depends on the friction model.

at $y=0$ outside the fault plane, we have:

$$u = 0 \quad (5)$$

$$w = 0 \quad (6)$$

$$\tau_{yy} = 0 \quad (7)$$

On the ground surface (free surface), we have:

$$\tau_{zx} = 0 \quad (8)$$

$$\tau_{zy} = 0 \quad (9)$$

$$\tau_{zz} = 0 \quad (10)$$

2 The finite element method

Using lumped mass finite element and central difference, Liao Z P [12, 13] has presented a time-space-decoupled, explicit finite element method to simulate wave motion. The key idea is to simulate wave motion locally, following actual wave traveling process. It does not need to consider stiffness of whole element in calculation at each step. Based on this idea, we can apply this explicit, decoupled technique to simulate dynamic rupture of earthquake source. For our problem, omitting the damping effect, to all nodes except nodes on the artificial boundary or at $y=0$, we have:

$$\mathbf{u}_i^{p+1} = 2\mathbf{u}_i^p - \mathbf{u}_i^{p-1} - \frac{\Delta t^2}{m_i} \sum_e \mathbf{k}_i^e \mathbf{u}^{e(p)} \quad (11)$$

Where \mathbf{u}_i is the node displacement, m_i is the lumped mass to the node i , Δt is the computational time step, e is the number of element which include node i , and \mathbf{k}_i^e is the stiffness matrix of an element which include node i . The superscript $p-1$, p , and $p+1$ represent three time steps during calculation, respectively. From formula (11), we notice that it needs not to use the displacement of whole nodes, when computing the displacement of node i at time $p+1$. The displacement of node i can be acquired through few elements stiffness and their nodes displacement at time p and $p-1$.

We use the multi-transmitting boundary formula [13] to obtain displacements of artificial boundary, as shown in formula (12),

$$u_B^{p+1} = \sum_{j=1}^N (-1)^{j+1} C_j^N u[x_B - jC_a \Delta t, t - (j-1)\Delta t] \quad (12)$$

where u_B^{p+1} is displacement of node X_B at artificial boundary at $p+1$ time step, C_a is artificial velocity, C_j^N is the binomial coefficient:

$$C_j^N = N! / [(N-j)! j!] \quad (13)$$

N is order taking in MTF. Formula (12) means displacements at artificial boundary can be obtained by those of inner nodes at pass time steps easily. The details of this scheme can be found in Ref. [12, 13].

On the fault plane and outside the plane (plane ADHE in Figure 1), we use the same method as given in formula 2.5 of Miyatake [10].

3 Validation of the method

In order to validate our finite element and multi-transmitting boundary technique, we compare numerical results with the Kostrov's (1964) [5] self-similar problem of a rupture initiate at a point and expanding with a constant speed as a circle over a plane in a full space. In Figure 1, we presume the rupture initiate at point O (in this case, we put the coordinate origin O far from the ground surface, in order to ensure the free surface reflect wave can not attain the fault upper boundary), and take the initial tectonic stress as 20Mpa and parallel to axis X, the dynamic frictional stress as 10Mpa. The density of the rock is $2.75 \times 10^3 \text{ kg/m}^3$, the shear velocity is 3200m/s, and the medium is Poisson solid. The Kostrov's self-similar solution is

$$u_x = c(v/\beta) \frac{\sigma_e}{\mu} \beta \sqrt{t^2 - r^2/v^2} H(t - r/v) \quad (14)$$

where $c(v/\beta)$ is a constant computed by Dahlen[6], v is rupture velocity, β is the S-wave velocity, r is the distance to the initial rupture point, $H(t)$ is the Heaviside step function, and σ_e is the stress drop. For this example, taking a rupture velocity such that $v = 0.9\beta$, $c(v/\beta)$ should be 0.81 according to Dahlen.

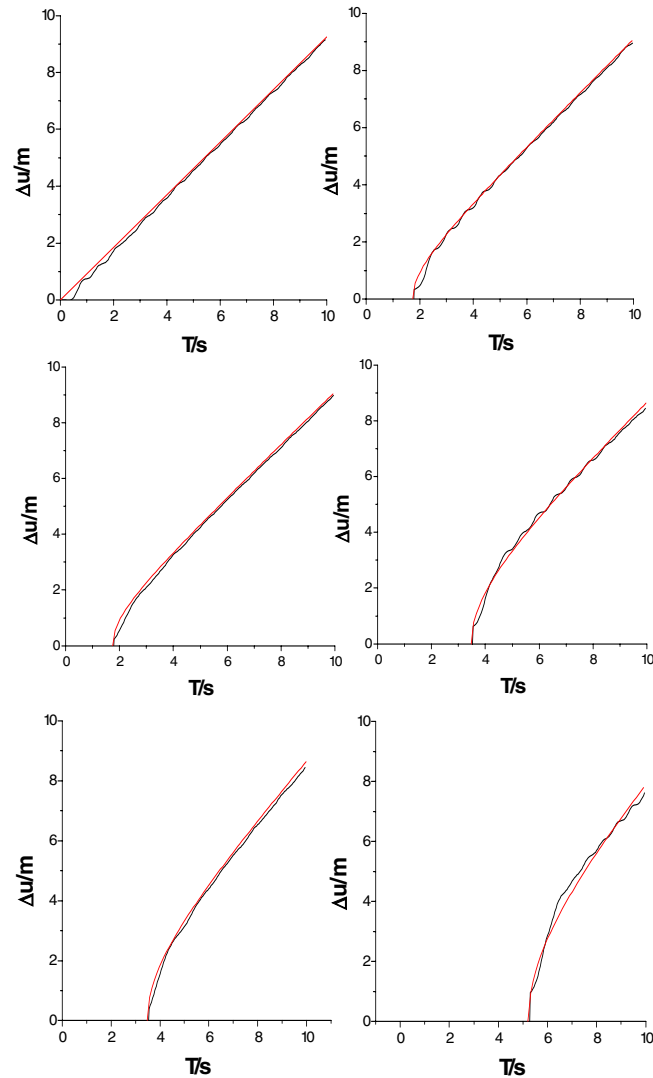


Figure 2 the solution of this paper (black line) and that of the Kostrov's self-similar solution (red line). The left top one is of the point $[0,0,0]$, The left middle one is of the point $[5,0,0]$, The left down one is of the point $[10,0,0]$, The right top one is of the point $[0,5,0]$, The right middle one is of the point $[0,10,0]$, The right down one is of the point $[0,15,0]$.

Figure 2 shows the analytical and numerical simulation results for six points at position $(0,0,0)$, $(5,0,0)$, $(10,0,0)$, $(15,0,5)$, $(0,0,5)$ and $(0,0,10)$ on the fault plane. The numerical results (black lines) agree quite well with the analytical results (red lines), which indicate that our finite element method can be used to simulate fault rupture accurately. Here, we take the rupture radius is 15 km. we have selected the computation area as $x=[-20,20]$, $x=[-25,25]$, $y=[0,-5]$, $y=[0,-10]$, $y=[0,-15]$, $z=[-20,20]$, $z=[-25,25]$ in order to clarify the efficiency of multi-transmitting boundary method. Those curves of all computational model are the superposition completely in Figure 2 (black line), which indicate that the multi-transmitting boundary works well in this problem.

THE EFFECT OF SLIP WEAKENING DISTANCE d_c ON SOURCE TIME FUNCTION AND NEAR FAULT GROUND MOTION

Some previous studies have shown that the friction properties between two sides of the fault controls earthquake rupture propagation. Some friction models have been proposed to describe friction law of earthquake fault [7, 8]. Here, we want to use our method to study the effect of slip weakening distance d_c on low frequency source function and near-field ground motion. The slip-weakening model used here is present firstly by Andrews (1976) and shown in Figure 1 of reference [8].

We take a vertical fault with length of 20km and width of 10km embedded within a half space, and the fault intersects the ground surface. The uniform initial tectonic stress is 20Mpa and parallel to axis X, and the dynamic frictional stress is 10Mpa. The density of the rock is $2.7 \times 10^3 \text{kg/m}^3$, the shear velocity is 3460m/s, and the medium is a Poisson solid. Assuming the rupture initiate from the fault center, and using finite stress strength criteria [1], we simulate a spontaneous rupture process and the low frequency near-field ground motion up to 1 Hz in this paper. Such low frequency strong ground motions are important because most structures are sensitive to stress period longer than 1 sec.

In order to study the effect of d_c to the source time function and near-field ground motion, we tested four models with constant strength excess and different d_c , the parameters of the models are list in table 1.

Table 1 the parameters of model with constant yield strength and different d_c

Model	τ_0 /mpa	τ_y /mpa	τ_f /mpa	S	d_c /m	G_c /J/m ²
I	20	25	10	0.5	0	0
II	20	25	10	0.5	0.2	1.5×10^6
III	20	25	10	0.5	0.5	3.75×10^6
IV	20	25	10	0.5	1.0	7.5×10^6

Where $s = \frac{\tau_y - \tau_0}{\tau_0 - \tau_f}$, G_c is the apparent fracture energy, and $G_c = \frac{1}{2}(\tau_y - \tau_f)d_c$.

Figure 3 shows the source dislocation function, the slip velocity function and its Fourier spectra of point on the upper and central line of the fault. Due to the symmetry of the problem (see Ref. 4), we only give the results of points of (0,0,-5), (2,0,-5), (4,0,-5), (6,0,-5), (8,0,-5) on the fault upper line and points of (0,0,0), (2,0,0), (4,0,0), (6,0,0), (8,0,0) on the fault center line. In these Figures, the black line is the result with slip weakening distance 0.1mm, the red line is the same with slip weakening distance 0.1mm, and the green line is the same with slip weakening distance 0.1mm.

Here, we noticed:

At the same point, while d_c is lager, the rupture will start later. Since the three models have the same yield stress, the fracture energy G_c will increase as d_c increases, and the rupture velocity will decrease as the slip weakening distance d_c increase.

- (1) Once d_c is larger than a certain value, the rupture can not extend (in this particular case, we found the rupture can not extend if d_c is larger than 1.2m).
- (2) The dislocation will decrease little as d_c increase. While d_c is smaller, the slip velocity pulse will be higher and the pulse width will be narrower.
- (3) For different d_c , although the fracture energy is very different, the Fourier spectra of slip velocity are very similar in this frequency range (0-1Hz), which means the low frequency (<1Hz) source time function is not sensitive to the rupture process.

Figure 4 and 5 shows the displacement, velocity histories and its velocity Fourier spectra for X and Y components at points 500m and 5km distance to the fault on the ground surface, respectively. Here, we noticed:

- (1) The ground residual displacements are almost identical for the entire four models, which mean the ground residual displacement is not affected by slip weakening distance d_c . It only depends on the stress drop and the medium parameters, not on the rupture process.

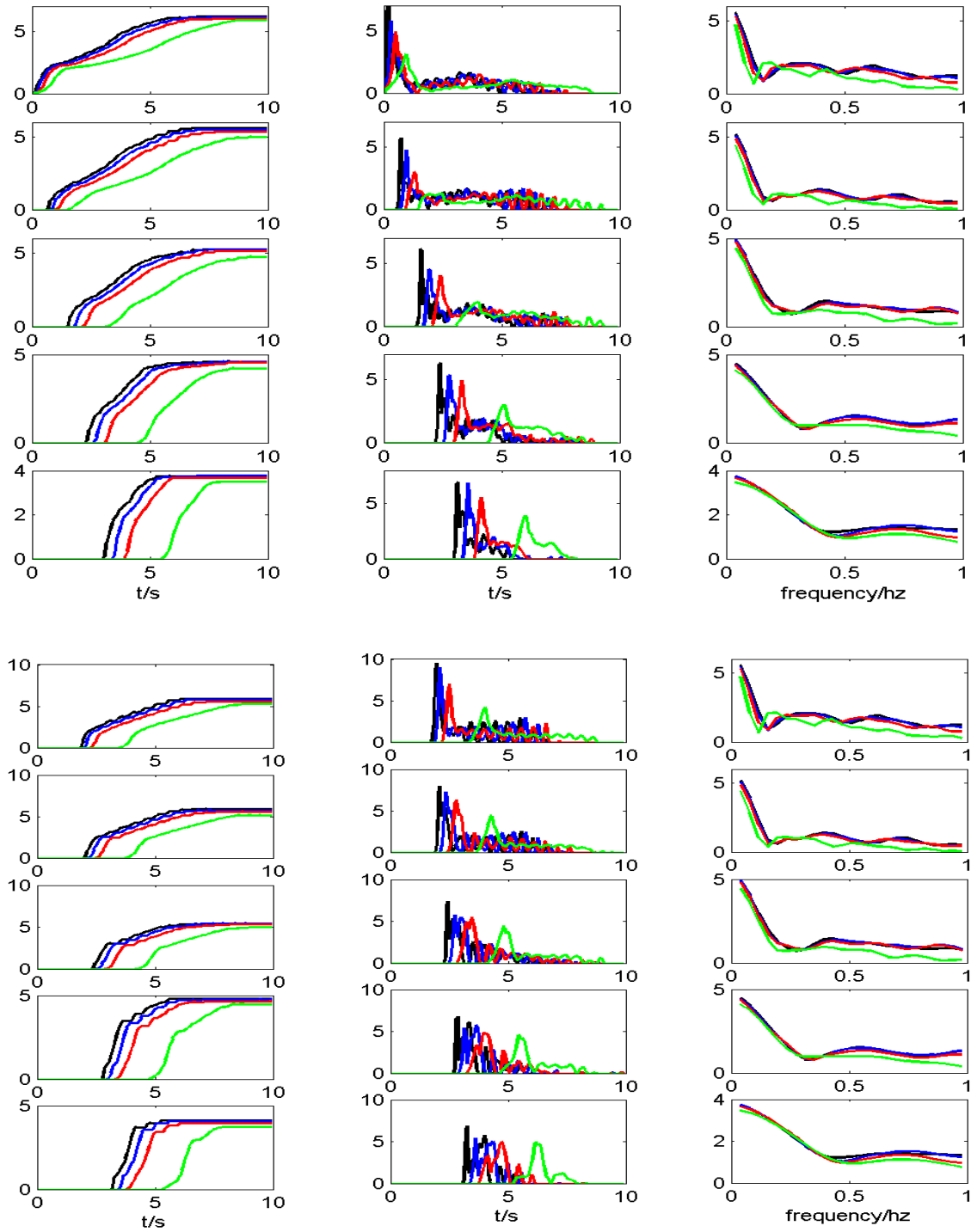


Figure 3 the dislocation (left column), the slip velocity (middle column) and the Fourier spectra of the slip velocity (right column) of points on the fault central line and on the fault upper line. From top to bottom row, the points coordinate are $(0,0,0)$, $(2,0,0)$, $(4,0,0)$, $(6,0,0)$, $(8,0,0)$, $(0,0,0)$, $(2,0,0)$, $(4,0,0)$, $(6,0,0)$, $(8,0,0)$, respectively. In this figure, the unit of dislocation is m, the unit of slip velocity is m/s, and the unit of slip velocity Fourier spectra is m.

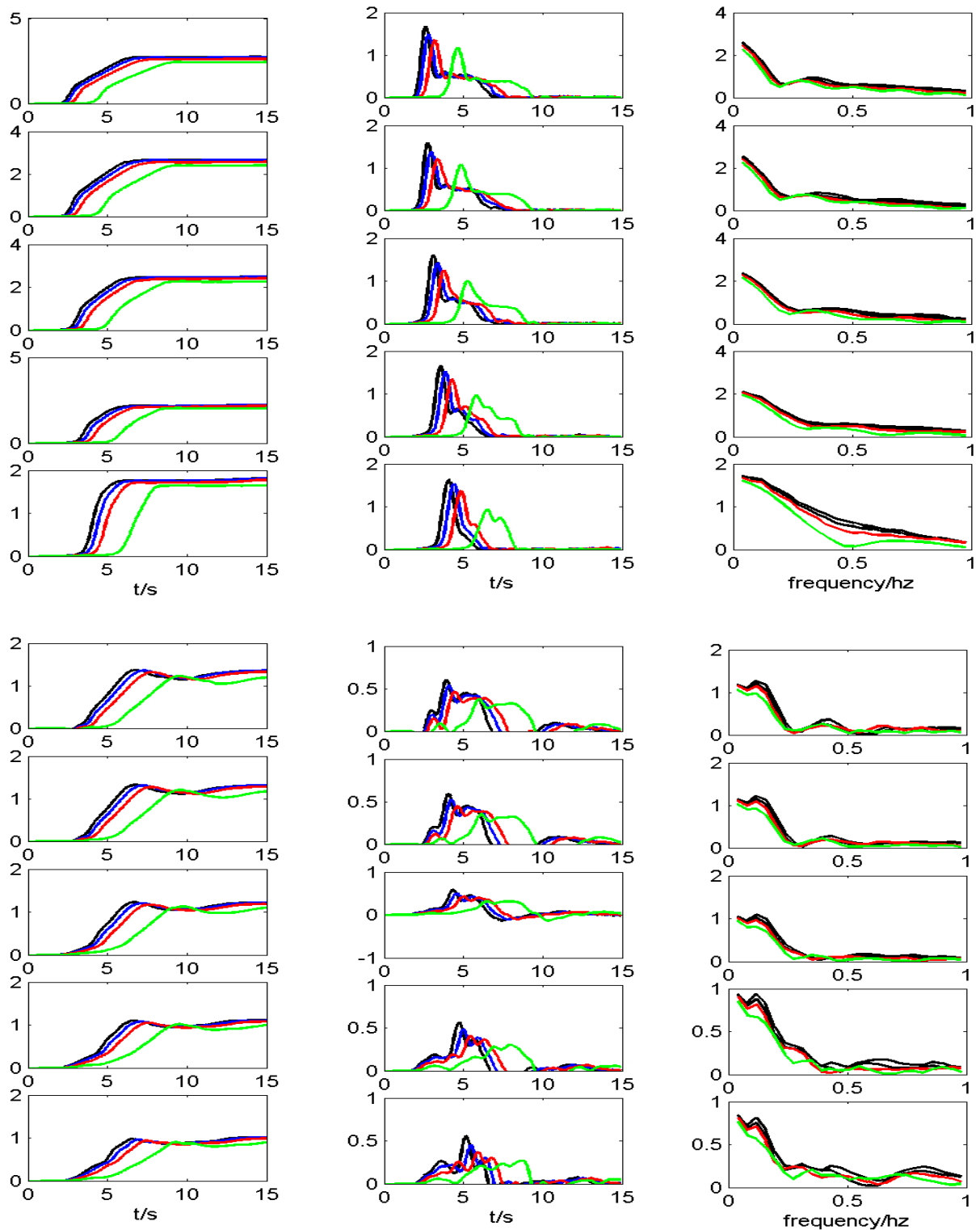


Figure 4 the displacement (left column), velocity (middle column) and the velocity Fourier spectra (right column) of X component of points 500m and 5km distance to the fault on ground surface. From top to bottom row, the points coordinate is (0,-0.5,-5), (2,-0.5,-5), (4,-0.5,-5), (6,-0.5,-5), (8,-0.5,-5), (0,-5,-5), (2,-5,-5), (4,-5,-5), (6,-5,-5), (8,-5,-5), respectively. In this figure, the unit of displacement is m, the unit of velocity is m/s, and the unit of velocity Fourier spectra is m.

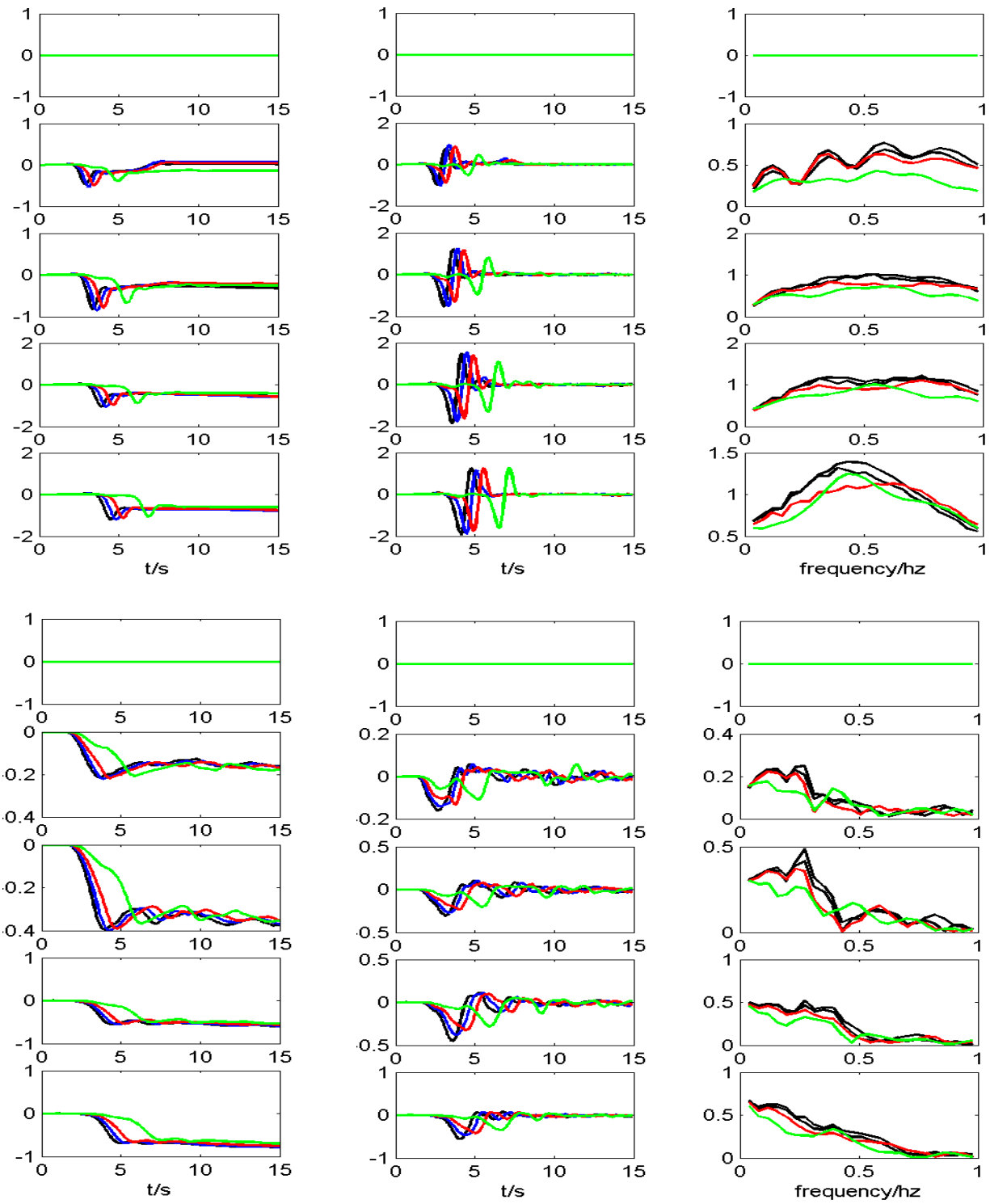


Figure 5 the same as Figure 4 except that of y component.

- (2) The slip velocity decreases as the slip weakening distance d_c increases.
- (3) For the displacement of X components, the Fourier spectra of slip velocity are very similar, except in some points when d_c is very large, while to Y component, the difference is a little larger.

Guatteri *et al* [14] have simulated two models with different d_c and strength excess, and their results are similar to ours in this low frequency range.

CONCLUSIONS AND DISCUSSIONS

We present a time-space-decoupled, explicit finite element method with multi-transmitting formula to simulate dynamic rupture process and its near-field ground motions. High efficiency can be obtained from this method by reducing computational storage and discrete model size in simulation.

By this method, we simulate a spontaneous rupture with different slip weakening distance d_c to study its effect on source function and velocity Fourier spectra. Interestingly, the results show both the low frequency source time function and the near field ground motions are not sensitive to d_c . The results are similar with that of Guatteri *et al*.

ACKNOWLEDGEMENT

This research is supported by National Natural Science Foundation of China under grant No.50378087.

REFERENCES

1. Das, S. and K. Ak (1977). A numerical study of two-dimensional spontaneous rupture propagation. *Geophys. J.* 50,643-668
2. Madariaga, R.(1976). Dynamics of an expanding circular fault. *Bull. Seism. Soc. Am.* 66, 639-666.
3. Archuleta, R. and G.A. Frazier (1978). Three-dimensional numerical simulation of dynamic faulting in a half-space. *Bull. Seism. Soc. Am.*, 68, 541-572.
4. Argaard B T, Hall J F, Heaton T H (1999). Characterization of near-source ground motions with earthquake simulations [J]. *Earthquake Spectra*, 17(2): 177~207.
5. Kostrov, B. V (1964). Self-similar problems of propagation of shear cracks, *J. Appl. Math. Mech.*, 28, 1077-1087
6. Dahel, F. A. (1974). On the ratio of P-wave to S-wave corner frequencies for shallow earthquake sources. *Bull. Seism. Soc. Am.* 64, 1159-1180.
7. Ida, Y.(1972). Cohesive force across the tip of a longitudinal-shear crack and Griffith's specific surface energy. *J. Geophys. Res.* 77, 3796-3805.
8. Andrews, J. (1976). Rupture velocity of plane strain shear cracks. *J. Geophys. Res.* 81, 5679-5687.
9. Burridge, R. and J. R. Wills. (1969). The self-similar problem of the expanding elliptical crack in an anisotropic solid. *Proc. Camb. Phil. Soc.* 68, 443-468
10. Miyatake, T. (1980). Numerical simulation of earthquake source process by a three-dimensional crack model. Part I, rupture process. *J. Phys. Earth.* 28, 565-598.
11. Madariaga, R. (1998). Modeling dynamic rupture in a 3d earthquake fault model. *Bull. Seism. Soc. Am.* 88, 1182-1197.
12. Liao Z. P. (1998). The decoupling numerical simulation of wave motion, in *Dynamic Soil-Structure Interaction* (ed. Zhang, Ch. Wolf J. P.), Amsterdam, 125-140.
13. Liao Z. P.(1996). Normal transmitting boundary condition, *Science in China, Series E*, 39(3), 244-254.
14. Gutteri, M., and P. Spudich.(2000). What can strong-motion data tell us about slip-weakening fault-friction laws? *Bull. Seism. Soc. Am.* 90, 98-116.